Synthesis of RGO/CF/PANI Magnetic Composites for Effective Adsorption of Uranium

Tran Quang Dat[ID], Nguyen Tran Ha[ID], Pham Van Thin, Nguyen Vu Tung, and Do Quoc Hung

Le Quy Don Technical University, Hanoi 122121, Vietnam

In this paper, adsorbents composed of reduced graphene oxide–$CoFe_2O_4$ ferrite–polyaniline (RGO/CF/PANI) nanocomposites have been synthesized by different techniques, namely, hydrothermal, graphite exfoliation, reduction, and polymerization. The adsorbents were characterized by scanning electron microscopy, X-ray diffraction, Fourier transform infrared spectroscopy, and vibrating sample magnetometer. The adsorption of uranium (VI) could be well described by the Langmuir and the pseudosecond-order models. The highest adsorption capacity of the composites for uranium (VI) was evaluated to be 2430 mg/g at pH = 5 and 25 °C. The uranium loaded RGO/CF/PANI could be readily separated from aqueous solutions by an external magnetic field. This paper demonstrates an efficient and convenient approach for the adsorption of uranium (VI) from aqueous solutions.

Index Terms—Adsorption, $CoFe_2O_4$, polyaniline (PANI), reduced graphene oxide (RGO), uranium.

I. INTRODUCTION

URANIUM is a standout amongst the most hazardous contaminants as a consequence of its long half-life time, high radiological, and organ-system toxicity [1]. Accordingly, it is vital to develop a suitable and efficient technique to isolate uranium from an aqueous medium. Along with other methods to remove uranium from aqueous solutions, adsorption has pulled in most intrigue in light of its cost-viability, adaptability, and straightforwardness of operation to separate uranium [2].

At present, significant attention has been paid to conducting polymers. They possess interesting, excellent chemical, opto-electronic, and electrical properties, thanks to the existence of special broaden π-conjugated electron frameworks [3]. Generally, conductive polymer is a hot topic in material science. However, conducting polymers involving polypyrrole, polyphenylene, polythiophene, polyaniline (PANI), polyacetylene, etc., have been broadly studied for the applications in other interdisciplinary research [4]. Among the conductive polymers, PANI has been most attractive due to its simple synthetization techniques, improved stability, outstanding electrochemical properties, lower cost, high thermic substantiality, and substantial quantities of utilizations [5]. Notwithstanding, PANI experiences numerous downsides, for example, bringing down dissolvability in ordinary solvents, poor cycling dependability, poor effectual surface territory, and degrading mechanical performance [6].

Incorporation of PANI with graphene-based material can improve the properties of PANI, since graphene is a liberal carbon-based material which is chemically and mechanically steady and has substantial operative surface area [7]. Exceptionally strong sorption of uranium onto graphene oxide (GO) can be referred with different functional groups (epoxide, phenol, hydroxyl, and carboxyl groups) on the surface of GO and expansive π-stacking that gives suitable interaction through hydrogen bonding, π–π, and electrostatic interactions [8]. However, the GO–PANI composites are hard to isolate from the aqueous solution after the adsorption process, and hence, segregation of uranium directly by using GO–PANI in industry might not be cost-effective.

Furthermore, as of the latest advances in the field, adsorbents pulled in more consideration from scientists as a type of material to remediate the encompassing water contamination due to the prospect of their partition from a fluidic medium by the utilization of external magnetic fields [9]. Separation of magnetic adsorbents by magnetic fields is quicker and more favorable than regular separation methods, for example, filtration, centrifugation, or sedimentation. Therefore, the composite materials, which consist of magnetic nanoparticles, GO, and PANI, will hold a promising perspective as effective adsorbents [10].

In this paper, we report the effortless synthesis method of ternary nanocomposite composed of RGO/CF/PANI. The synthesized nanocomposite was used as an adsorbent for effective adsorption of uranium ions [U(VI)] from the aqueous solution.

II. EXPERIMENTAL SETUP

A. Reagents and Chemicals

Analytical grade chemicals were used. Cobalt(II) nitrate hexahydrate [$Co(NO_3)_2 \cdot 6H_2O$, 99%], iron(III) chloride hexahydrate ($FeCl_3 \cdot 6H_2O$, 99%), sodium hydroxide (NaOH, 99%), ammonia (NH_3, 25%), ammonium persulfate [$(NH_4)_2S_2O_8$, 98%], nitric acid (HNO_3, 65%), hydrochloric acid (HCl, 37%), and uranyl nitrate hexahydrate [$UO_2(NO_3)_2 \cdot 6H_2O$, 99%] were supplied by Sigma-Aldrich company. All solutions were prepared with deionized water (DI).

B. Synthesis of RGO/CF/PANI Materials

Reduced GO (RGO) was received following the previous report [11]. To synthesize RGO/CF composite, first, 4 mmol of

FeCl$_3 \cdot$6H$_2$O and 2 mmol of Co(NO$_3$)$_2 \cdot$6H$_2$O were dissolved in a mixture of 60 mL of ethylene glycol and 40 mL of DI water. A solution which contained RGO (100 mg RGO/10 mL water) was slowly added to the mixture and stirred for 1 h. After that, 4 mL of ammonia solution was slowly added to the mixture. The mixture was stirred for 4 h for achieving good uniformity. The obtained mixture was poured into a 150-mL Teflon-lined autoclave reactor and heated to 190 °C. The reactor was kept at that temperature for 24 h. In the wake of cooling to room temperature, the precipitate was washed repeatedly using water and ethanol. Then, RGO/CF sample was dried at 60 °C for 12 h.

The RGO/CF/PANI composite was synthesized by polymerization of aniline monomers on the surface of RGO/CF. Beforehand, a mixture containing aniline and RGO/CF was prepared by dissolving 2 mmol of alinine in 70 ml of 28.5% HCl solution and kept cold at 0 °C. This precooled solution was added appropriately to RGO/CF powder. Then, 30 mL of aqueous solution containing 2 mmol of ammonium persulfate was added dropwise into the prepared mixture. The polymerization reaction was sustained for 16 h at 0 °C with energetic mechanical stirring at about 400–500 rpm. After that, the RGO/CF/PANI composite was taken out from the reaction mixture and repeatedly washed with water and ethanol. At the end of the washing cycle, RGO/CF/PANI composite was isolated from the solution by using an external magnet. Washing cycle was repeated until the filtrate became colorless. The obtained product (RGO/CF/PANI powder) was dried in vacuum at 60 °C for 24 h in a vacuum oven.

C. Characterization of Materials

The morphologies and crystal structures of the composites were characterized using scanning electron microscopy (SEM–S4800), X-ray diffraction (XRD, Bruker D5 with Cu K$_{\alpha 1}$ radiation $\lambda = 1.54056$ Å), and Fourier transform infrared spectroscopy (FTIR, Perkin Spectrum Two). Magnetic measurements were performed with a vibrating sample magnetometer (VSM, DMS 880 in magnetic fields of up to 13.5 kOe).

D. Adsorption Experiments

A batch technique was carried out to study the adsorption of U(VI) from aqueous solutions by RGO/CF/PANI. Uranium solutions used in all adsorption experiments were prepared by dissolving UO$_2$(NO$_3$)$_2 \cdot$6H$_2$O in DI water. All the adsorption experiments were performed at 25 °C and 20 mg of adsorbent was used in each experiment. After the adsorption reached the equilibrium, the adsorbent was separated from the solution by a magnet. It took a few minutes to conduct this experimental step. Then, the samples were filtered and the uranium concentration of the effluent was measured by inductively coupled plasma mass spectrometry (ICP-MS, Agilent 7500). The effect of pH on adsorption was studied using a 400-mL solution (50 mg/L uranium), a contact time of 240 min. The pH values ranging from 2 to 10 were adjusted by adding 0.1 mol/L NaOH or 0.1 mol/L HNO$_3$ solution. The effect of contact time on adsorption capacity was studied using 400-mL solution
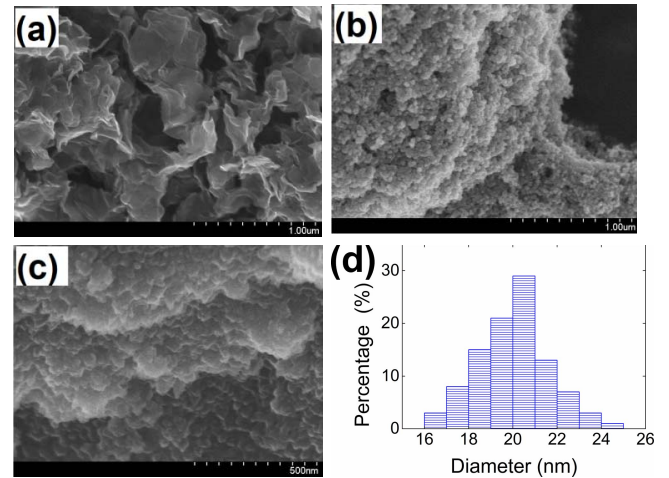

Fig. 1.   SEM image of (a) RGO, (b) RGO/CF, (c) RGO/CF/PANI, and (d) particle size distribution of CF.

(50 mg/L uranium) and pH = 5. The contact time varied from 15 to 360 min. In the adsorption equilibrium isotherm studies, the initial concentrations of uranium were varied and the other parameters were kept constant ($V_{\text{solution}} = 400$ mL, contact time = 240 min, and pH = 5).

The amount of uranium adsorbed per unit mass of the adsorbent was calculated according to the following equation:

$$Q_e = \frac{C_o - C_e}{m} V \qquad (1)$$

where Q_e (mg/g) is the adsorption capacity, C_o and C_e (mg/L) are the concentrations of the uranium at initial and equilibrium states, respectively, m is the weight of sorbent (g) and V is the volume of the solution (L).

The regeneration–reuse studies were carried out in eight cycles. 20 mg of adsorbent was mixed in a 400-mL uranyl solution (50 mg/L) in each cycle. Adsorption of U(VI) was performed at pH = 5, contact time = 240 min, and 25 °C. After the adsorption experiment, derived sample of U(VI) laden with RGO/CF/PANI composites was mixed with 0.1 mol/L of HCl for 2 h at 25 °C. The composites were separated by a magnet. The recovered composite materials were washed carefully few times with distilled water and dried at 50 °C. The adsorption efficiency in each cycle was calculated from the amount of uranium adsorbed on the adsorbents and the initial amount of uranium.

III. DISCUSSION

A. Morphology, Structure Characterization, and Magnetic Properties of Composites

According to Fig. 1(a), the thin RGO leaves were separated from graphite, but they were strongly deformed and wrinkled. Fig. 1(b) shows the SEM image of the RGO/CF composite. In accordance with it, the CF particles disperse well and cover almost totally the whole surface of the RGO, so that the RGO leaves cannot be seen except only at the boundaries between the RGO/CF blocks.

Fig. 1(c) shows the surface morphology of the composite RGO/CF/PANI. After the aniline monomers are polymerized,
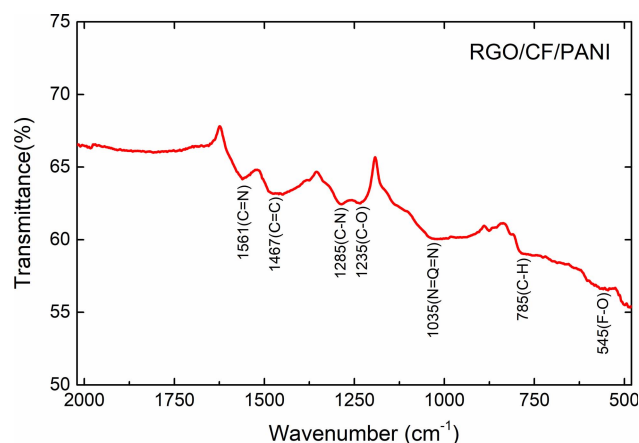
Fig. 2. FTIR spectra of RGO/CF/PANI.

Fig. 3. XRD patterns of (a) RGO/CF and (b) RGO/CF/PANI.

the polymer should cover roughly the thorough surface of the RGO/CF. And in the SEM image, we could not distinguish RGO/CF blocks, but RGO/CF/PANI layers could be seen quite evidently. In the SEM image of RGO/CF, only the most clear-cut particles were used to calculate the particle size. The CF particle size distribution is shown in Fig. 1(d). In the figure, it can be seen that the particle sizes range from 16 to 25 nm in diameter. The distribution curve has a typical bell-shape with the maximum in the range of 19–21 nm.

The surface functional groups of the synthesized materials were investigated with FTIR spectroscopy. Fig. 2 shows the FTIR spectrum of the RGO/CF/PANI material. The peak at 1561 cm^{-1} could be assigned corresponding to the (N = Q = N) vibrations of quinonoid-rings. The peak at 1467 cm^{-1} corresponds to the (C = C) in the vibrations of benzenoid rings [12]. The presence of quinoid and benzenoid units indicates the conductive emeraldine form of PANI. A peak at 1285 cm^{-1} can be accredited to the C–N stretching vibration. The peaks at 1235 and 1035 cm^{-1} correspond to the vibrations of C–O bonds [13]. The peak at 785 cm^{-1} corresponds to vibrations of C–H bonds. Also, the appearance of characteristic peak at 545 cm^{-1} corresponds to Fe–O bond stretching [14]. These peaks show the interactions that appear in the material.

In the XRD pattern of the RGO/CF [Fig. 3(a)], we can see peaks corresponding to the (220), (311), (400), (422), (511), and (440) crystal planes, respectively. XRD data identified that the CF particles have a face-centered cubic trevorite structure. The crystallite size of the CF nanoparticles was evaluated using the Scherrer formula: $d = k\lambda/\beta \cdot \cos\theta$, where k is equal to 0.94, λ is the X-ray wavelength, β is the peak full width half maximum, and θ is the diffraction peak position. Results obtained by calculation with the (311) peak display that the crystallite size of CF in RGO/CF composite is 20 nm. This data is in great correspondence with the previous analysis of the SEM image. In the XRD pattern of RGO/CF/PANI, it is difficult to realize peaks of CF particles because of the covering PANI layer. Otherwise, a broad peak at about 25.5°, which corresponds to interlayer spacing of RGO, can be seen.

Room temperature magnetization of the RGO/CF/PANI composite was studied and the result is presented in Fig. 4.
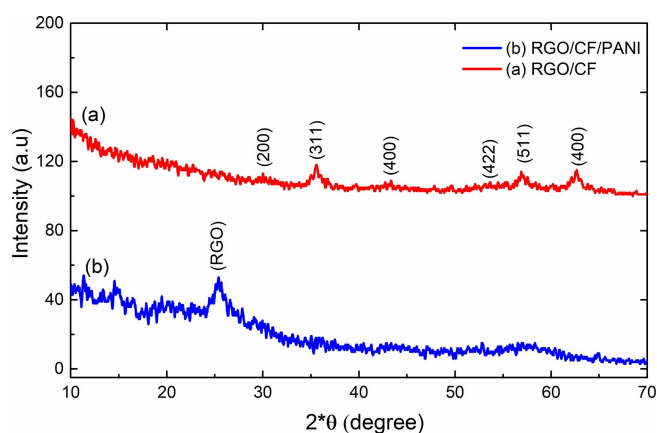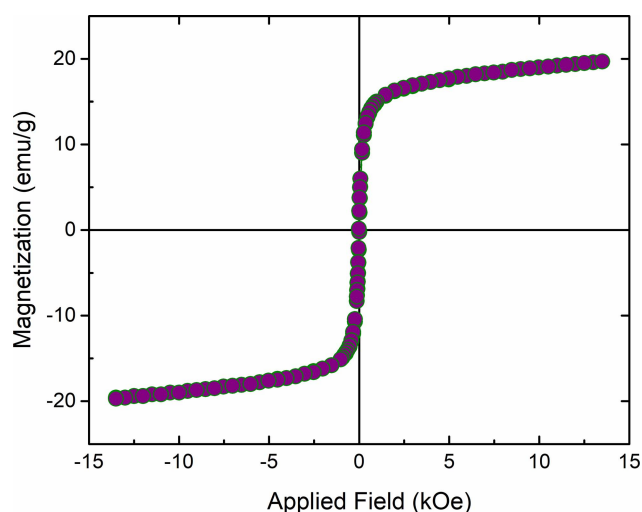

Fig. 4. Room temperature magnetic hysteresis loops of RGO/CF/PANI.

The VSM measurement demonstrated that achieved materials were generally superparamagnetic-like with remanences and coercive forces near zero. The maximum magnetization value of the RGO/CF/PANI is about 20 emu/g. In our experiments, the RGO/CF/PANI sample have 50 wt% of $CoFe_2O_4$. The saturated magnetization of our $CoFe_2O_4$ is 40 emu/g. The present results are in good agreement with previous experiments.

B. Effect of pH

The pH of the sample solution is an important factor to control the sorption efficiency uranium. The effect of pH on the amount of uranium adsorbed on the RGO/CF/PANI composite for U(VI) is carried out in Fig. 5. The amount of uranium is augmented when the pH increases from 2 to 5. As the pH value is reliably extended from 5 to 10, the amount of adsorbed U(VI) diminishes. This result demonstrates that the sorption capacity of RGO/CF/PANI for U(VI) reaches its best value when pH = 5.

In acidic mediums, U(VI) is in the form of UO_2^{2+} and the sorption is small as the result of the competition of UO_2^{2+} with H^+ ions for the coupling sites of the adsorbents.
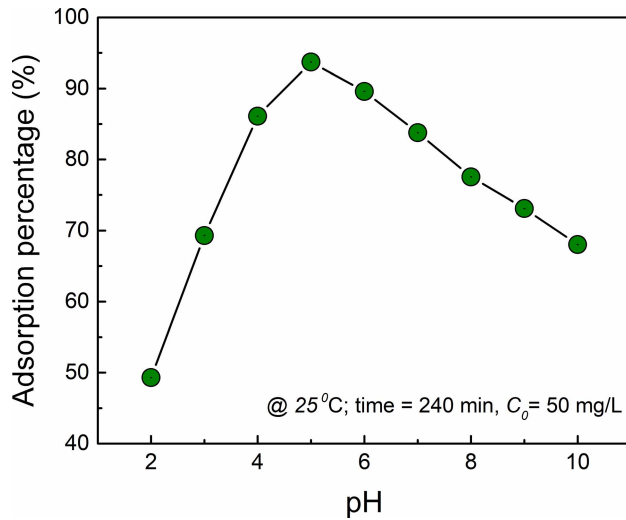
Fig. 5.   Effect of pH on uranium adsorption.

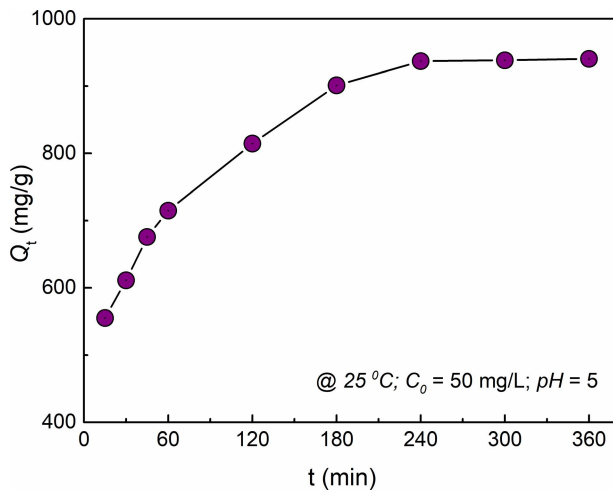Fig. 7.   (a) Pseudofirst- and (b) second-order plot for the uranium adsorption.

Fig. 6.   Effect of contact time on uranium adsorption.

The concentrations of hydroxyl, carbonate, and bicarbonate anions expand alongside pH level. Therefore, the uranyl ions form stable complexes with hydroxyl and carbonate anions, bringing about a dramatic diminishing in adsorption capacity [15]. At pH > 5, the surface charge of sorbents become more negative and uranium appears as anionic species such as $[UO_2(OH)_3]^-$ and $[UO_2(OH)_4]^{2-}$. The electrostatic repulsion between uranium anions and sorbents with surface negative charges that tends to decrease the U(VI) adsorption [16].

C. Effect of Contact Time

Influence of contact time on adsorption is shown in Fig. 6. According to Fig. 6, two specific stages are appeared in this adsorption. The first process was completed in around 240 min. The last process was slow and extended to 360 min. Moreover, the uranium adsorption onto RGO/CF/PANI reached up to 93.7% within 240 min and was almost constant thereafter. Hence, the contact time of 240 min was chosen
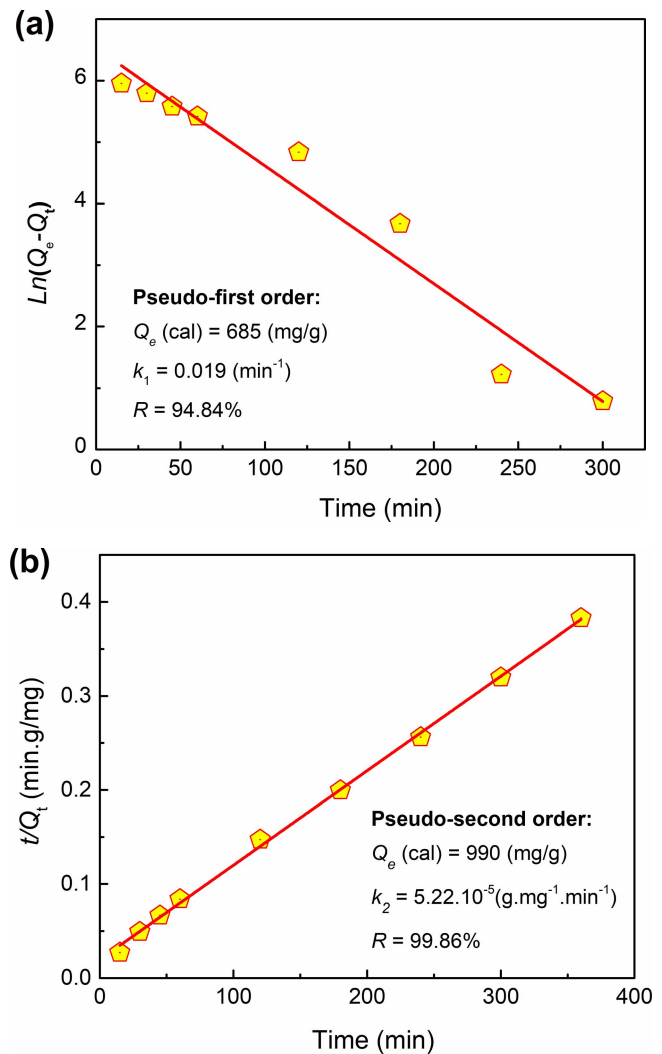
for all adsorption experiments to confirm that equilibrium was set up in each adsorption process. This contact time is similar to some other studies, but has a lower adsorption capacity [16]–[19]. The adsorption kinetics curves were studied to determine the kinetic parameters and models which well fit these experimental data. To this purpose, the adsorption of uranium on RGO/CF/PANI nanocomposite with respect to time was treated in terms of the pseudofirst-order or pseudosecond-order kinetic models [20]. The best model was selected by evaluating the correlation coefficient values (R^2), experimental capacity at equilibrium time ($Q_{e,exp}$), and calculated capacity ($Q_{e,cal}$).

As shown in Fig. 7, the pseudosecond-order kinetic model is found to have higher correlation coefficient and its R^2 value is closer to unity than that of the pseudofirst-order kinetic model. Moreover, the amount of uranium calculated by the pseudosecond-order kinetic equation is in good agreement with the experimental values. It can be inferred that the sorption kinetics of uranium (VI) by the RGO/CF/PANI adsorbent can be well explained in terms of the pseudosecond-order kinetic model.
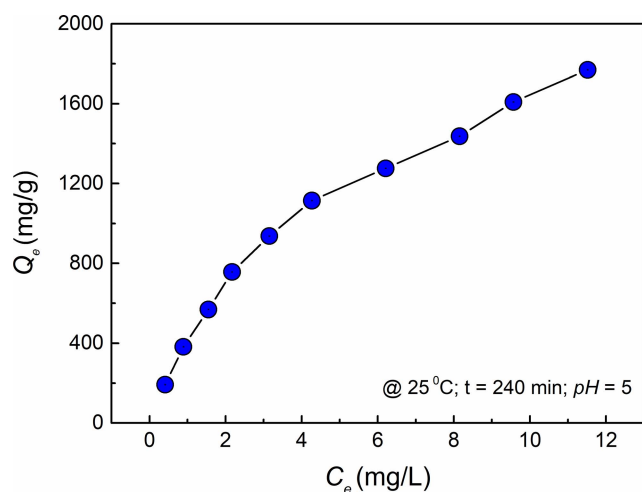
Fig. 8.   Effect of equilibrium uranium on the adsorption.

D. Adsorption Isotherms of Uranium

The adsorption experiments at different initial concentrations of U(VI) were carried out to estimate the influence of equilibrium concentration as presented in Fig. 8. Obviously, increasing the uranium concentrations involves an increase in the uptake of uranium. The sorption isotherm gives the most important information, as it indicates how the sorbent molecules are distributed between the solid and the liquid phases when the sorption process reaches its equilibrium state. The removal of uranium in the presence of materials can be allocated to the interaction between material surface and uranium species presented in the solution. A maximum sorption amount of U(VI) on ternary nanocomposite (RGO/CF/PANI) was found to be 1770 mg/g in our experimental conditions. It is considered that RGO/CF/PANI has high capacity of U(VI) sorption exhibited a potential of utilization in removal and recovery of uranium from aqueous solutions.

Langmuir and Freundlich isotherms were applied for the experimental determination of adsorption correlation parameters which are used to determine the adsorption pattern and capacity [9]. Plots of Langmuir and Freundlich models representing uranium adsorption are delineated in Fig. 9. In light of the high correlation coefficient value, the Langmuir isotherm can be more suitable to characterize the uranium adsorption behavior of the RGO/CF/PANI materials. The Langmuir model shows that uranium is adsorbed by particular locales of RGO/CF/PANI and forms a homogeneous monolayer. According to the Langmuir isotherm, maximum adsorption capacity of RGO/CF/PANI is around 2430 mg/g for uranium at 25 °C. The adsorption capacity of the RGO/CF/PANI composite is higher than that of some other adsorbents (Table 1).

The RGO/CF/PANI materials have some kind of sorption centers and sites (due to nano sizes of ferrite particles, high specific surface area, and RGO–ferrite interactions). In addition, on surface of the material there are many complex groups such as $S-NH_2$, $S = NH$, and $S-COOH$ (where S is the surface). Uranium ions in solution could be interacted with these complex groups through electrostatic or hydrogen
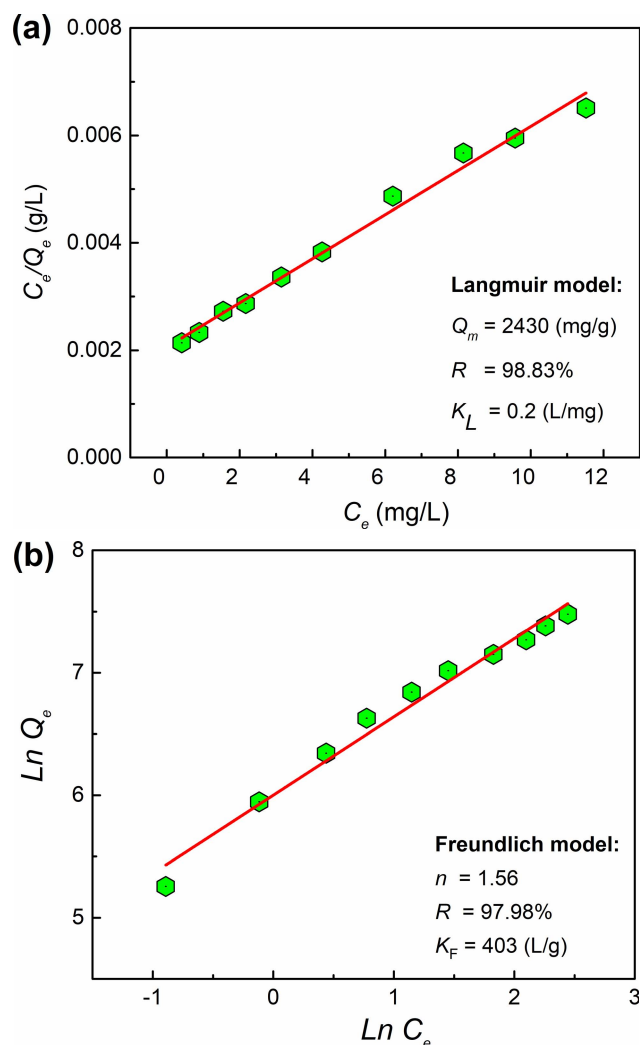

Fig. 9.   Sorption isotherms for the uranium adsorption. (a) Langmuir. (b) Freundlich.

TABLE I
ADSORPTION CAPACITY OF DIFFERENT ADSORBENTS
FOR URANIUM (VI)

Adsorbents	Capacity (mg/g)	pH	Ref
$Fe_3O_4@TiO_2$ core-shell	91	6	[19]
RGO/Fe_3O_4	97	7	[21]
Amidoxime - $Fe_3O_4@SiO_2$	119	7	[22]
Fe_3O_4-Oxine	125	7	[18]
$CoFe_2O_4$ hollow	170	6	[9]
$CoFe_2O_4$/Graphene	227	6	[16]
Graphene oxide sheets	299	4	[17]
Fe^0/PANI/Graphene	350	5.5	[15]
$RGO/Zn_{0.5}Ni_{0.5}Fe_2O_4$/PANI	1885	5	[10]
PANI/GO	1960	6-7	[8]
$RGO/CoFe_2O_4$/PANI	2430	5	This work

bond [8]. So, the adsorption capacity of this adsorbent could be improved.

E. Regeneration–Reuse Studies

The reusability of the adsorbent is an important feature for applied application and must be scientifically studied.
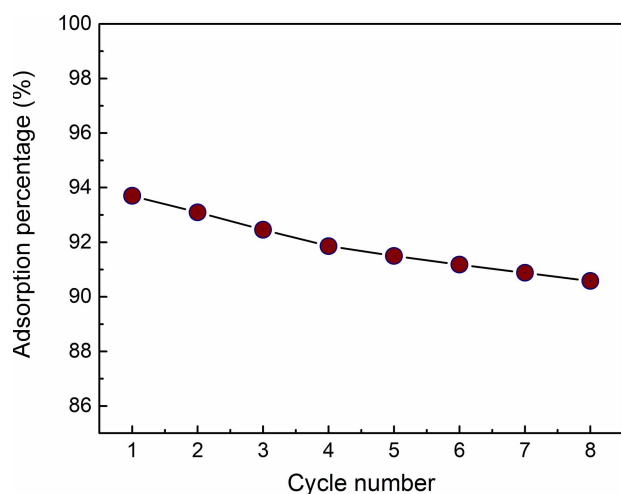
Fig. 10. Adsorption–desorption cycles for uranium of RGO/CF/PANI.

Fig. 10 demonstrates that the reusability of RGO/CF/PANI for the adsorption of U(VI) in eight cycles. There is minor reduction in the adsorption percentage of the adsorbent after each repeated cycle because of the unperfected desorption of U(VI) from the surface of the adsorbent. The adsorption percentage decreased just slightly from 93.7% to 90.6% after eight cycles. These results point out the way to increase the cost-effectiveness of the adsorption process. Similar results were also reported for reusability of other U(VI) adsorbents [8], [9], [18], [19]. With that in mind, RGO/CF/PANI composite materials stand out as a suitable adsorbent for wastewater treatment application.

IV. CONCLUSION

The RGO/CF/PANI nanocomposite was successfully synthesized and used as an adsorbent for adsorption of uranium from polluted water. The nanocomposites were characterized by SEM, FTIR, XRD, and VSM. The isotherm and kinetic studies showed that the Langmuir isotherm and pseudosecond-order models well described the experimental data. The maximum uranium adsorption capacity of the RGO/CF/PANI composite was estimated to be 2430 mg/g at pH = 5 and 25 °C within the Langmuir model. The RGO/CF/PANI composite appears as an effective uranium-adsorbent holding promising application in U(VI) segregation from aqueous solution in the view of their simplicity of magnetic separation and high adsorption capacity.

ACKNOWLEDGMENT

REFERENCES

[1] M. Majdan, S. Pikus, A. Gajowiak, D. Sternik, and E. Zięba, "Uranium sorption on bentonite modified by octadecyltrimethylammonium bromide," *J. Hazard. Mater.*, vol. 184, nos. 1–3, pp. 662–670, Dec. 2010.

[2] P. D. Bhalara, D. Punetha, and K. Balasubramanian, "A review of potential remediation techniques for uranium(VI) ion retrieval from contaminated aqueous environment," *J. Env. Chem. Eng.*, vol. 2, no. 3, pp. 1621–1634, Sep. 2014.

[3] G. Kaur, R. Adhikari, P. Cass, M. Bown, and P. Gunatillake, "Electrically conductive polymers and composites for biomedical applications," *RSC Adv.*, vol. 5, pp. 37553–37567, Apr. 2015.

[4] S. Shahabuddin, N. M. Sarih, S. Mohamad, and S. N. A. Baharin, "Synthesis and characterization of Co_3O_4 nanocube-doped polyaniline nanocomposites with enhanced methyl orange adsorption from aqueous solution," *RSC Adv.*, vol. 6, pp. 43388–43400, Apr. 2016.

[5] P. Zhang, X. Han, L. Kang, R. Qiang, W. Liu, and Y. Du, "Synthesis and characterization of polyaniline nanoparticles with enhanced microwave absorption," *RSC Adv.*, vol. 3, pp. 12694–12701, May 2013.

[6] J. Luo, W. Zhong, Y. Zou, C. Xiong, and W. Yang, "Preparation of morphology-controllable polyaniline and polyaniline/graphene hydrogels for high performance binder-free supercapacitor electrodes," *J. Power Sour.*, vol. 319, pp. 73–81, Jul. 2016.

[7] S. Mondal, U. Rana, and S. Malik, "Reduced graphene oxide/Fe_3O_4/polyaniline nanostructures as electrode materials for an all-solid-state hybrid supercapacitor," *J. Phys. Chem. C*, vol. 121, no. 14, pp. 7573–7583, Feb. 2017.

[8] D. Shao, G. Hou, J. Li, T. Wen, X. Ren, and X. Wang, "PANI/GO as a super adsorbent for the selective adsorption of uranium(VI)," *Chem. Eng. J.*, vol. 255, pp. 604–612, Nov. 2014.

[9] J. Wei, X. Zhang, Q. Liu, Z. Li, L. Liu, and J. Wang, "Magnetic separation of uranium by $CoFe_2O_4$ hollow spheres," *J. Chem. Eng.*, vol. 241, pp. 228–234, Apr. 2014.

[10] T. Q. Dat, P. T. Hung, and D. Q. Hung, "Efficient removal of uranium from aqueous solution by reduced graphene oxide-$Zn_{0.5}Ni_{0.5}Fe_2O_4$ ferrite-polyanilinenanocomposite," *J. Elect. Mater.*, vol. 46, pp. 3273–3278, Mar. 2017.

[11] T. Q. Dat, N. T. Ha, and D. Q. Hung, "Reduced graphene oxide-$Cu_{0.5}Ni_{0.5}Fe_2O_4$-polyaniline nanocomposite: Preparation, characterization and microwave absorption properties," *J. Elect. Mater.*, vol. 46, no. 6, pp. 3707–3713, Mar. 2017.

[12] X. Hong, B. Zhang, E. Murphy, J. Zou, and F. Kim, "Three-dimensional reduced graphene oxide/polyaniline nanocomposite film prepared by diffusion driven layer-by-layer assembly for high-performance supercapacitors," *J. Power Sour.*, vol. 343, pp. 60–66, Mar. 2017.

[13] B. Ramezanzadeh, M. H. M. Moghadam, N. Shohani, and M. Mahdavian, "Effects of highly crystalline and conductive polyaniline/graphene oxide composites on the corrosion protection performance of a zinc-rich epoxy coating," *J. Chem. Eng.*, vol. 320, pp. 363–375, Jul. 2017.

[14] K. Mohanraju, V. Sreejith, R. Ananth, and L. Cindrella, "Enhanced electrocatalytic activity of PANI and $CoFe_2O_4$/PANI composite supported on graphene for fuel cell applications," *J. Power Sour.*, vol. 284, pp. 383–391, Jun. 2015.

[15] L. Chen, S. Feng, D. Zhao, S. Chen, F. Li, and C. Chen, "Efficient sorption and reduction of U(VI) on zero-valent iron-polyaniline-graphene aerogel ternary composite," *J. Colloid Interface Sci.*, vol. 490, pp. 197–206, Mar. 2017.

[16] L. Tan *et al.*, "Uranium extraction using a magnetic $CoFe_2O_4$–graphene nanocomposite: Kinetics and thermodynamics studies," *New J. Chem.*, vol. 39, pp. 2832–2838, Feb. 2015.

[17] Z. Li *et al.*, "Uranium(VI) adsorption on graphene oxide nanosheets from aqueous solutions," *J. Chem. Eng.*, vol. 210, pp. 539–546, Nov. 2012.

[18] L. Tan *et al.*, "Facile preparation of oxine functionalized magnetic Fe_3O_4 particles for enhanced uranium (VI) adsorption," *Colloids Surf. A, Physicochem. Eng. Aspects*, vol. 466, pp. 85–91, Feb. 2015.

[19] L. Tan *et al.*, "Synthesis of Fe_3O_4@TiO_2 core–shell magnetic composites for highly efficient sorption of uranium (VI)," *Colloids Surf. A, Physicochem. Eng. Aspects*, vol. 469, pp. 279–286, Mar. 2015.

[20] T. S. Anirudhan, J. R. Deepa, and Binusreejayan, "Synthesis and characterization of multi-carboxyl-functionalized nanocellulose/nanobentonite composite for the adsorption of uranium(VI) from aqueous solutions: Kinetic and equilibrium profiles," *Chem. Eng. J.*, vol. 273, pp. 390–400, Aug. 2015. [Online]. Available: https://scholar.google.co.in/citations?user=Yzv82csAAAAJ&hl=en

[21] W. Cheng, Z. Jin, C. Ding, and M. Wang, "Simultaneous sorption and reduction of U(VI) on magnetite–reduced graphene oxide composites investigated by macroscopic, spectroscopic and modeling techniques," *RSC Adv.*, vol. 5, pp. 59677–59685, Jul. 2015.

[22] Y. Zhao *et al.*, "Synthesis of amidoxime-functionalized Fe_3O_4@SiO_2 core-shell magnetic microspheres for highly efficient sorption of U(VI)," *J. Chem. Eng.*, vol. 235, pp. 275–283, Jan. 2014.